Case Studies in Thermal Engineering 36 (2022) 102182

Contents lists available at ScienceDirect

Case Studies in Thermal Engineering

journal homepage: www.elsevier.com/locate/csite

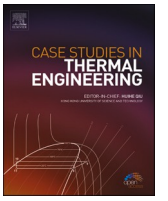

Towards compliance with the prospective EURO VII NOx emissions limit using a thermoelectric aftertreatment heater

J. Ximinis, A. Massaguer, E. Massaguer *

Department of Mechanical Engineering and Industrial Construction University of Girona, C. Universitat de Girona, 4, 17003, Girona, Spain

ARTICLE INFO

Keywords:
Thermoelectric generator
Exhaust gas heater
NOx reduction
Heavy duty vehicle
ATEG
EGH

ABSTRACT

In this study, the use of a thermoelectric aftertreatment heater (TATH) to reduce NOx emissions in low demanding regimes of diesel-powered Heavy-Duty vehicles (HDV) has been analysed. This system is composed by an Exhaust Gas Heater (EGH) that heats up the exhaust gases in low engine regimes, in order to shorten the time that urea is injected. Besides, the TATH is fed by an Automotive Thermoelectric Generator (ATEG) that converts the waste heat from exhaust gases into electricity, so the system can work energetically autonomous.

Experimental results show that under low-speed regimes, a Euro VI certified HDV emits NOx 5 times above the Euro VI limit value. Results demonstrate that the use of a TATH reduces NOx emissions by up to 97.2% in a long-haul diesel-powered MAN Euro VI TGX 18.480 Efficient Line 2 and may help to fulfil the prospective EURO VII regulation. Apart from that, it is also demonstrated that an ATEG can produce the energy required by the EGH in a long-haul mission profile. However, the added weight and the back pressure caused by the TATH is expected to increase the fuel consumption of the vehicle in 0.35%.

Abbreviations

ATEG	Automotive Thermoelectric Generator
ATS	Aftertreatment System
DEF	Diesel Exhaust Fluid
DOC	Diesel Oxidation Catalyst
DPF	Diesel Particle Filter
ECU	Electronic Control Unit
EGH	Exhaust Gas Heater
EGR	Exhaust Gas Recirculation
FTPP	Full Throttle Pedal Position
HDV	Heavy Duty Vehicle
ISC	In-Service Conformity
MAW	Moving Averaging Window
PEMS	Portable Emissions Measurement System
SCR	Selective Catalytic Reducer

* Corresponding author.
E-mail address: eduard.massaguer@udg.edu (E. Massaguer).

https://doi.org/10.1016/j.csite.2022.102182
Received 14 February 2022; Received in revised form 18 May 2022; Accepted 4 June 2022
Available online 7 June 2022

TATH	Thermoelectric Aftertreatment Heater
TEM	Thermoelectric Module
WHSC	World Harmonized Stationary Cycle
WHTC	World Harmonized Transient Cycle

Author statement

Joan Ximinis: Conceptualization, Methodology, Investigation, Writing-Original draft preparation. **Albert Massaguer:** Conceptualization, Investigation, Supervision, Writing-Review and Editing. **Eduard Massaguer:** Conceptualization, Supervision, Writing-Review and Editing.

1. Introduction

Heavy duty vehicles (HDVs) have been recognised the world over as significant contributors to air pollution. Current tier legislation for the type approval of motorized vehicles with regards to (pollutant) emissions was adopted in 2013 with Euro VI standard for heavy duty. It has been amended many times since then, culminating in 2020 with the current stage Euro VI-E (see Table 1).

Recently, the European Commission started the regulatory work aimed at setting the next stage of emissions standards, known as Euro 7 (for light-duty vehicles) and VII (for heavy-duty). The new Euro 7/VII, which will be presented during 2022 and expected to come into force on 2025 [1], will develop stricter CO_2 and NO_X limits, as well as new tests and limits for non-CO_2 greenhouse gas emissions [2]. There is no official information yet, but some reports have developed different scenarios pointing out that NO_X limits will be halved from Euro VI, placing the limit around 0.2g/kWh [3–6]. A briefing from T&E also suggests an introduction of a low speed test cycle to measure NOx in urban driving conditions without excessive Conformity Factors (CF) [7]. Taking these references in mind we propose a post Euro 6 scenario of halved limit values and a maintained CF as it is common for all vehicles since January 2021. Comparative figures can be seen in Table 1.

Since Euro VI, emissions have been tested through the World Harmonized Stationary Cycle (WHSC) and the World Harmonized Transient Cycle (WHTC). The Euro VI standards introduced off-cycle laboratory testing and on-road testing with portable emissions measurement systems (PEMS). The testing requirements for type-approval include: WHSC + WHTC test for diesel engines; WHTC test for positive ignition engines; Off-cycle emission testing over the WNTE control area of the engine map, and the on-road PEMS vehicle test. Additionally, the Euro VI regulation introduced in-service conformity (ISC) on-road PEMS testing.

A vehicle is deemed compliant if the average emissions, using the Moving Averaging Window (MAW) method, are below the ISC limit. The ISC limit is a function of the type-approval limit over the WHTC (0.46 g/kWh for Euro VI), multiplied by a conformity factor (ISC limit = 0.46 g/kWh·1.5 = 0.69 g/kWh). This calculation will be used to provide an analysis as close as possible for real-world driving conditions.

Although emission limits have been tightened and on-road measurements have been introduced, some studies point out that under specific engine regimes, emissions can exceed the regulatory limit. The aim of these experiments is not to replicate regulation conditions but to show that in some real driving conditions pollutants abatement must be improved.

Grigoratos et al. [8] tested five Euro VI diesel HDVs on-road under conditions that not necessarily comply with the official ISC test. They observed relatively high emissions for some of the pollutants over low-speed phases due to reduced effectiveness of the corresponding emission control systems. NOx emissions of the tested HDVs ranged from 0.1 to 2.05 g/kWh at low-speed regimes. One of these vehicles exceeded the Euro VI engine certification limit (0.46 g/kWh) by a factor of 1.7.

TNO reported that despite most Euro VI HDVs emit overall low NOx, in some cases under busy urban driving conditions they can emit NOx over the conformity level of 1.5 [9]. Furthermore, this study [10] confirmed this statement by measuring NOx emissions of eight N3 Euro VI trucks (tractor semi-trailers and one rigid with trailer) over real world conditions.

Bishop et al. [11] reported that a large percentage of vehicles observed at a low speed location in California have catalytic devices functioning below a minimum temperature threshold restricting thus the potential effectiveness of SCR systems to further reduce NOx emissions.

Vojtisek-Lom et al. [12] evaluated the prevalence of trucks with excess NOx emissions on Czech motorways using an ordinary Customs Administration patrol vehicle temporarily fitted with a portable fast-response Fourier Transform Infra-Red (FTIR) analyser,

Table 1
Comparative Euro standards for heavy duty diesel engines and proposed scenario.

Tier	Come into force	Stationary test		Transient test		
		Test	NO_X (g/kWh)	Test	NO_X (g/kWh)	CF
Euro III	October 2000	ESC + ELR	5.0	ETC	5.0	–
Euro IV	October 2005		3.5		3.5	
Euro V	October 2008		2.0		2.0	
Euro VI (Euro VI-E)	January 2013 (September 2020)	WHSC	0.4	WHTC	0.46	1.5
Euro VII[a]	2025	WHSC	0.2	WHTC	0.27	1.5

[a] Expected scenario. Euro VII emissions regulations for trucks and buses is ongoing.

acting as an impromptu chase vehicle. A total of 222 unique trucks were measured (66% were Euro VI). They found that about 10–25% of Euro VI trucks are believed to be excess emitters, with no SCR functionality on about 10–15% of Euro VI trucks.

Using on-board NOx sensor data from two diesel transit buses, Kotz et al. [13] showed that these buses emitted NOx at rates 3 to 9 times higher than the standard, primarily due to low load and low-speed operations. Tan et al. [14] reported the same.

Posada et al. [15] analysed five European trucks designed to meet the Euro VI NOx standard. The analysis finds that European HDVs are better designed than U.S. trucks to control NOx emissions under low-speed, low-load, and idle conditions. The U.S. HDVs studied emit on average 1.4 times more NOx per unit work than the European vehicles. During urban driving conditions, NOx emissions were twice as much as their total route emission values.

In this regard, the aforementioned studies demonstrate that certified HDVs emit NOx above the current regulation limit under certain conditions. However, this does not mean that they do not fulfil the corresponding regulation. The gap between real-world and certified NOx emissions is especially wide during urban driving conditions and other low-load operations in diesel HDVs.

This high NOx emissions at low-speed, low load and idling are due to the fact that the SCR does not reach high enough temperature (i.e.>180 °C) to effectively abate engine out NOx [8,16–19]. This occurs during cold starts and urban driving conditions, when the exhaust gas temperature is not high enough for SCR catalyst activation. Ammonia process reaction normally starts from 180 °C, achieving its maximum reaction value around 350 °C [20]. If exhaust gas temperature is roughly below 180 °C, generation of derivatives such as ammelide, biuret, cyanuric acid and melamine create deposits on pipe walls as a decomposition of urea [21], being counter-productive for regular gas flow [22]. In fact, urea addition generally starts with exhaust gas temperatures around 220 °C in order to avoid undesired products generation. Therefore, Euro VI certified HDVs may emit pollutants above the regulatory limits if operate frequently in suburban areas, where traffic is mainly managed with traffic signs (traffic lights, stop signals, etc …) and the speed rarely exceeds 50 km/h.

Posada et al. [15] observed that a disproportionate amount of NOx emissions from heavy-duty vehicles is emitted during the low-speed operation characteristic of urban driving. Vehicle operation at speeds of less than 40 km/h results in NOx emissions of more than five times the certification limit. Apart from that, a single line-haul truck emits the NOx equivalent of 100 cars for each mile driven in urban driving. Based on 160 tests with a Portable Emissions Measurement System (PEMS), this study also shows that these trucks, which are optimized for highway driving, spend on average 43% of their time and emit 40% of the total mass of NOx in urban-like operation, including low-speed driving and idling.

With the objective to improve SCR conversion during low-speed driving, some authors have studied the use of exhaust heaters. Some electrical preheated catalytic converters have been tested with relevant results [23,24]. However, this solution is not as efficient as heating the exhaust gases directly. Mera et al. [25] implemented a system composed of an electric heating SCR and demonstrated that SCR inlet gas heating at 200 °C had the best deNOx/CO_2 penalty trade-off. The minimum threshold of 200 °C resulted in the best NOx/CO_2 trade-off, reducing on average 4.7 mg of NOx per gram of CO. Culbertson et al. [26] studied the capability of an electric heater to effectively raise the temperature of the exhaust and avoid the effect of moisture in low exhaust temperature. This allowed NOx conversion to start earlier. Results demonstrated that it is possible to achieve high NOx conversion temperatures rapidly using robust heater technology for diesel applications. Sharp et al. [27] studied several options to reach extremely low NOx values on a 361 kW Volvo HDV with a conventional turbocharged engine. Researchers investigated an electrically heated catalyst of 2 kW, coupled to a hydrolysis catalyst alone or combined with an additional heater of 5 kW assembled after the DPF and upstream the DEF. This system was compared to a mini-burner with adjustable-power from 8 kW to 20 kW. These configured ATS can provide a 45%, 70% and 80% in overall tailpipe NO_x emissions reductions respectively. However, these operating systems represent an increase of energy consumption that has to be carefully quantified.

However, in these studies it is assumed that the energy consumed by electrical heaters comes from the vehicle's electrical system. Therefore, to proceed to an overall evaluation, the impact of such systems on fuel consumption and overall vehicle efficiency must be addressed [19].

Massaguer et al. [28] proposed the use of an Automotive Thermoelectric Generator (ATEG) coupled to an Exhaust Gas Heater (EGH). This system could reduce up to 97% the NOx emitted during cold starts. The ATEG is used to transform waste thermal energy, afterwards the aftertreatment system, into electrical energy. The electricity generated is stored in a battery to be used by the EGH. This energy will be used when the EGH is required to heat the exhaust gas in low engine regimes, in order to shorten the time that urea is injected and reduce NO_x emissions. This EGH + ATEG system, also known as Thermoelectric Aftertreatment Heater (TATH), is developed to be energetically closed avoiding direct extra consumption of fuel for its use.

Recently, a new study [19] has experimentally demonstrated that a TATH could produce 80% NOx emissions reduction in a Euro VI HDV at low engine regimes without the need of using extra energy. It also represents an improvement on SCR efficiency up to 55% for low engine regimes. The proposed system can be retrofitted in any Euro VI truck, which means that it can be installed without the need of replacing the existing aftertreatment system.

The objective of the present study is to assess whether a TATH allows a diesel-powered MAN TGX HDV Euro VI to emit NOx below the current Euro VI and VII limits for low demanding regimes.

To carry out this study, the vehicle will be subjected to different working conditions on a dynamometer roller bench to obtain the emission map under standard operation. The test will be repeated with the inclusion of an EGH before the ATS. NOx reduction will be analysed with respect to the standard version without EGH. This study will determine which is the power required by the EGH to emit NOx below Euro VI and Euro VII limits. Finally, an ATEG will be sized to ensure that the system can work electrically autonomous. The power consumption of auxiliary equipment, the additional back pressure caused into the exhaust pipe and the additional weight on the vehicle will be considered.

2. Thermoelectric aftertreatment heater

As stated before, the proposed system retrofits into the standard ATS two main components: the ATEG, located downwards the ATS, and the EGH, located upstream of the ATS. Fig. 1 shows a detailed scheme of the exhaust pipe with the standard ATS and the proposed TATH. The estimated total weight of the TATH system (i.e. EGH, ATEG, battery and electronic system) is around 60 kg.

Considering the exhaust gas flow, each component of the proposed TATH is assembled to maximize its functionality. The EGH is located after the turbocharger and the EGR valve. This element is assembled backwards the standard ATS of the vehicle, composed of a diesel oxidation catalyst (DOC), a diesel particle filter (DPF), a SCR and a diesel exhaust fluid (DEF) dosing system. The location of the EGH is crucial to help the standard NO_x reduction equipment as it provides higher exhaust gas temperature with minimal thermal loss. Despite the ideal location of the EGH is just before the SCR, it was impossible to achieve as the vehicle treated in this paper mounted a compact ATS (i.e. DOC, DPF and SCR in the same compartment).

Exhaust gas temperature is reduced while ATEG is converting energy by the thermoelectric effect. This is exactly the opposite of what ATS needs. Taking this into account, the ATEG must be assembled afterwards the ATS.

As can be seen in Fig. 1, the ATEG is complemented with a cooling system composed by a radiator and a hydraulic pump. Thermoelectric systems need to be cooled to achieve high temperature differences between hot and cold sides of thermoelectric modules (TEM). The lower the cooling temperature, the higher the efficiency of the ATEG [29]. In this study, the ATEG makes use of a refrigeration system independent of the vehicle to keep it cold. The additional power consumed by the hydraulic pump is supplied by the ATEG. The radiator is cooled by the flow of air onto it when the vehicle is in motion. Neither the aerodynamic loss due to the increased heat-exchanger surface of the radiator nor the hydraulic pressure loss in the refrigeration circuit have been considered.

The energy generated by the ATEG is send to the battery charging regulator (REG). To recover the maximum energy from exhaust gases, it is best to use a REG equipped with a maximum power point tracking system (MPPT) [30].

The additional weight of the system together with the additional exhaust pressure loss must be properly considered. We must take into account that the inclusion of the TATH cause a backpressure (BP) increase in the exhaust system. These effects will be analysed in chapter 5.

The TATH is designed to work in two different stages:

- **Heating stage:** in this stage the control unit (CONT) uses the energy stored into the battery to feed the EGH, which is used to rise the temperature of exhaust gases. The purpose of this stage is to rapidly heat the exhaust gases just before SCR. This stage begins when the engine starts, and it is maintained as long as the temperature of exhaust gases is lower than the light-off SCR temperature (i.e. $<$180 °C). Reaching this target temperature as quick as possible is its main goal. When exhaust gases reach this point, urea solution could be dosed into the system causing a drastically abatement of NOx. Time invested during this phase is related to achieve target temperature ($=$180 °C). As it is demonstrated in the following chapter, exhaust temperatures of a MAN TGX HDV Euro VI are significantly lower than light-off temperature for regimes around 1000 rpm ($\sim 55 km/h$). Therefore, the heating stage will only take place at speeds below 55 km/h.
- **Recovery stage:** the recovery stage aims to charge the electrical battery with the residual heat from exhaust gases. This power will be used by the EGH during heating stage, mainly at low engine regime conditions. The ATEG is the responsible of converting waste heat into electricity during the operation of the vehicle. Unlike heating stage, which only takes place at certain moments along the way, the recovery stage lasts as long as the vehicle is running, even during the heating stage. It begins as soon as the engine is started and can last 270 min (equalling the maximum continuous drive time of 4.5 h). As stated in other studies, the generated power of the ATEG (P_{ATEG}) increases directly with the engine regime as exhaust temperatures are higher at high engine regimes [29, 31]. In consequence, the difference of temperature between the hot side and the cold side of each thermoelectric module (TEM) increases, $\Delta T = T_{HOT} - T_{COLD}$. If we consider $P_{ATEG} \propto \Delta T^2$, it can be stated that increasing engine regime, increases the ATEG generated power. Besides, the longer the mission time, the higher the energy recovered by the ATEG. In conclusion, the most suitable HDV to incorporate a TATH are long-distance transport vehicles.

To achieve emissions reduction without direct extra fuel consumption, a balance between energy consumed (heating stage) and produced (recovery stage) must be achieved. In this regard, the mission profile of the HDV will play an important role in the TATH viability. A heavy-duty vehicle used in urban or suburban deliveries will spend the major part of its time at low-speed regimes. Mainly

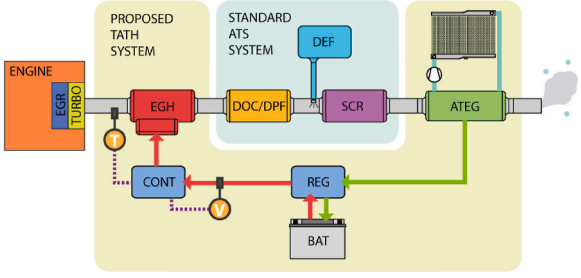

Fig. 1. Proposed TATH system with the electrical energy flows: heating stage (red) and recovery stage (green). (For interpretation of the references to colour in this figure legend, the reader is referred to the Web version of this article.)

because traffic flow on urban and suburban routes has its speed limited around 50 km/h and is frequently interrupted and delayed by traffic lights, stop signs, and intersections. This would cause the EGH to demand more energy than the ATEG could supply, making the use of TATH unviable. Contrarily, a long-haul HDV travels the major part of its time on highway at high engine regimes. Its speed profile is much more stable and closer to the highway limit speed, around 80 km/h.

Fig. 2 shows a 266min long-haul mission profile of a HDV. Note that the vehicle spends $t_{HIGH} \approx 262min$ on highway conditions and just $t_{SUB} \approx 4min$ on suburban conditions. With long periods of time traveling in highway and interurban roads, the recovery stage can last long enough to store the energy required for the heating stage. This reason explains why in this study a long-haul HDV has been chosen as the target vehicle of the TATH.

To study the technical feasibility of the TATH system, two experiments were designed: the EGH and the ATEG experiment. The EGH experiment was designed to study the effect of an EGH for NOx emissions abatement. The ATEG experiment was designed to obtain the power generated by an ATEG under real exhaust conditions of temperature and mass flow in a HDV.

Two separate experiments were carried out due to the lack of information to correctly size the entire system. Note that at the beginning of the study we did not know what power the EGH needs to reduce NOx emissions nor what power must be generated with ATEG to compensate the energy consumed by the EGH. The results of this study will allow us to size the complete system in a more efficient way in a future work. These two experiments are explained in detail in the following chapters.

3. EGH experiment

3.1. EGH experiment set up

The most restrictive antipollution standard for HDV in the EU is the Euro VI standard, currently active. However, details of Euro VII (the next standard) will be announced during 2022 and probably come into force in 2025. To cut NO_x ppm values below Euro VI limits, manufacturers rely on a combination of a catalytic reaction system together with sophisticated ECU (Electronic Control Unit) software. In this study, a Heavy-Duty Vehicle Euro VI TGX 18.480 Efficient Line 2 from MAN was used to carry out the tests. Its most relevant characteristics are shown in Table 2.

The whole system was disposed as presented in Fig. 3. A certified test bench for testing HDVs (Maha Powerdyno R200/1) was used to put the vehicle in real operating conditions. This equipment was also used to capture the Full Throttle Pedal Position (FTPP), NOx after and before the ATS, and exhaust temperatures from the ECU. Unfortunately, the on-board acquisition system specifications were not available, so the accuracy of its measures is unknown. The EGH power consumption was measured by a power meter. Type K thermocouples were used as temperature probes for exhaust gas temperature measurement. A specific sensor was located at the end of the exhaust pipe to register NO_x emissions. Specifications are listed in Table 3.

To prevent rear wheel sliding, the rolling bench was preloaded before testing. The same load was used in all tests within the experiment. To avoid gas flow alterations, the EGH was installed preserving the original exhaust pipe and minimizing its deviation. Two thermocouples measure temperatures before EGH ($T_{B_{EGH}}$) and after the EGH ($T_{A_{EGH}}$), both fundamental parameters to study the whole performance of the ATS.

The selected EGH was a Watlow ECOTEG unit with a maximum heating power of 12 kW. This component contains an electric heating coil externally powered by a three-phase circuit and controlled by a temperature regulation system (CONT) that adjusts the power injected to the EGH according to the temperature set point (i.e. 300 °C). Note that the power consumed by the EGH to heat the fumes up to SCR light-off temperature depends on the exhaust gas conditions. As explained in the results chapter, the power consumed by the EGH ranges from 4 to 10 kW. Selected key parameters such as NOx ppm, temperatures or engine regime, were synchronized, monitored, and registered.

Downwards the exhaust pipeline, it follows a compartment shared by a DOC and a DPF. The first one is responsible for the oxidation of carbon monoxide (CO) and unburned hydrocarbons (HC). Besides, it provides a permanent regeneration of the DPF and contributes

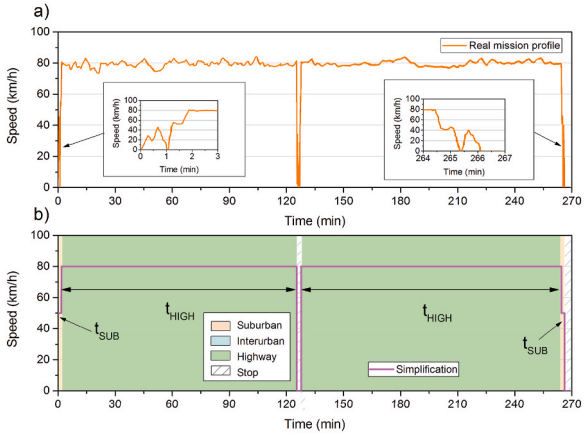

Fig. 2. a) Speed profile of a long-haul heavy-duty vehicle [8]. b) Simplified speed profile.

Table 2
Main specifications of tested vehicle.

Parameter	Value
Maker	MAN
Model	TGX 18.480 Efficient Line 2
Gearbox	Automatic (12 gears)
Max. rated power	353 kW (at 1800 rpm)
Max. rated torque	1500 Nm (at 930–1400 rpm)
Emission standard	Euro VI

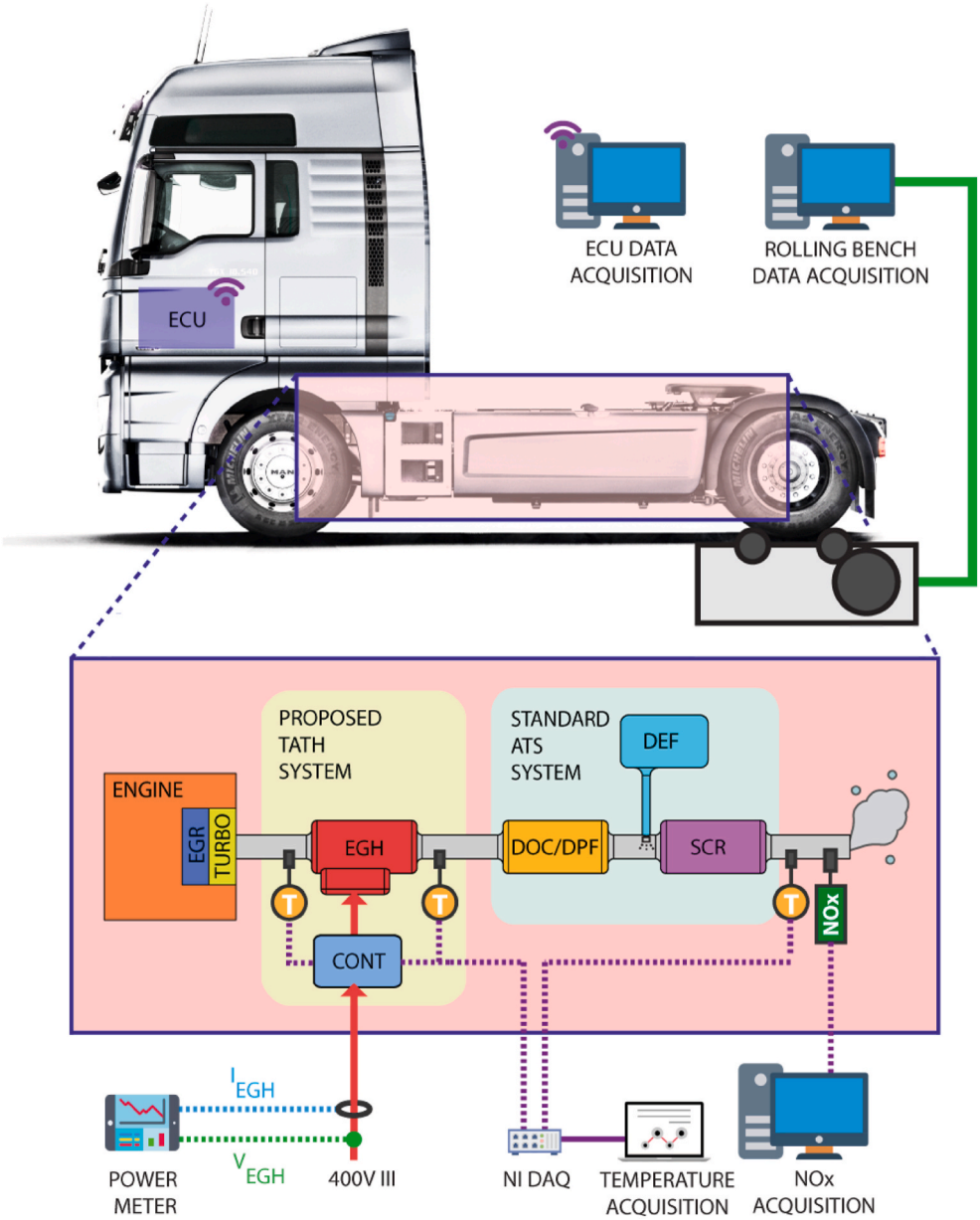

Fig. 3. Scheme of the EGH experiment with data acquisition modules.

to its better performance capturing even the smaller organic fraction (OF) of diesel particles. Soot is also trapped in the filter surface and it is burned when maximum backpressure is reached. The induced regeneration injects more fuel to rise exhaust gases temperature and burn the undesired particles. Threshold value is fixed by each manufacturer.

Table 3
Equipment specifications and its measurements.

EQUIPMENT	MODEL	SPECIFICATIONS/ACCURACY
Power meter	Dranetz Power Explorer PX5	Measured current: from 1 to 6000 Arms with 0.1% rdg + CTs (4) Measured voltage: from 1 to 600 Vrms with 0.1% rdg (reading) + 0.05% FS (full scale) 256 samples/cycle and 16-bit ADC
Data acquisition system	National Instruments DAQ	NI 9211 acquisition module Type K thermocouples Maximum measure error: 2.2 °C (0–400 °C) Measurement sensitivity: <0.07 °C
NOx sensor	MIAC G4.0	Measure range: 0 to +5000 ppm Resolution: 0.1 ppm (0 to +500 ppm) Accuracy: ±5 ppm (0 to +99.9 ppm) and ±5% of mv (+100 to +2000 ppm)

In second place of the standard ATS system, there is a package of components related to the Diesel Exhaust Fluid (DEF) function. This set includes the fluid tank and the supply and dosing modules. The mentioned fluid is a commercial urea solution which is injected into the system after exhaust gas temperature is over 180 °C. DEF management is controlled by ECU parameters specifically designed for this vehicle. The dosing module is connected to temperature and NO_x sensors (one installed before the DOC and another located after the SCR) providing real time precise dose of urea solution to fulfil a particular standard (i.e. Euro VI). Finally, the exhaust gases combined with this solution enter the SCR (Selective Catalytic Reduction) unit. A catalytic reaction is produced inside to transform NOx into water (H_2O) and diatomic nitrogen (N_2).

The main parameters acquired are: the FTPP, the engine torque, the vehicle speed and the SCR inlet temperature, which are necessary to carry out the subsequent analysis. Other data, like the EGH inlet temperature ($T_{B_{EGH}}$), the outlet temperature ($T_{A_{EGH}}$), the heater electrical power consumption ($P_{EGH} = \sqrt{3} \cdot V_{EGH} \cdot I_{EGH} \cdot \cos\varphi$ being V_{EGH} the voltage and I_{EGH} the current) and the NO_x emissions (NOx_{EGH}) are obtained using other external equipment. A scheme of these acquisition modules is also shown in Fig. 3.

With this combined ATS layout, a SCR efficiency increase is expected in cold start conditions and low demanding urban routes. Besides, to minimize alterations of exhaust gas temperatures, the best location for the ATEG is afterwards the SCR.

The experiment is divided into three different stationary points. To achieve all FTPP range the eleventh gear was selected. In each particular test, point data has been registered only after achieving the desired stationary regime. In order to maintain the same engine conditions during all tests, engine coolant temperature has been kept below 90 °C, replicating nominal working conditions. Consequently, short periods of time between tests were required to cool down the engine temperature. Table 4 shows all regimes selected for this experiment. All of them can be found in a typical daily drive.

3.2. EGH experimental results

To analyse if the incorporation of an EGH is beneficial or not for the abatement of NOx emissions, two NOx emissions maps are confronted in Fig. 4. On one side, Fig. 4a shows the NOx emissions map of a MAN TGX 18.480 Efficient Line 2 Euro VI HDV with its standard ATS (i.e. EGH was disabled). On the other side, Fig. 4b shows the NOx emissions map of the same vehicle but with the EGH enabled. On both maps the boundary regions for compliance with the Euro VI and Euro VII limits have been marked as orientation zones. According to Table 1, these limits have been calculated from the ISC limit, as the result of the WHTC value multiplied by the conformity factor CF: $NOx_{limit}^{EURO\ VI} = 0.46 \cdot 1.5 = 0.69 g/kWh$ and $NOx_{limit}^{EURO\ VII} = 0.27 \cdot 1.5 = 0.41 g/kWh$.

From Fig. 4a, it can be observed that under certain engine regimes, mainly low-speed regimes, a Euro VI certified HDV emits NOx pollutants above the limit value. This agrees with what authors in Refs. [8–11] observed. The highest NO_x emissions appear at regimes around 1000 rpm, which correspond to suburban driving conditions. The highest value is located at 1000 rpm and 60% FTPP, where NOx emission reach 3.83 g/kWh. Note that at this regime this value can exceed the regulation limit but the vehicle can still fulfil the corresponding EURO regulation. In mid demanding regimes, such as 1200 − 1500 rpm, is where EGH is less required because the engine produces enough heat to reach the SCR light-off temperature and make the catalytic conversion highly efficient [19]. Note how the over-emission area grows with the inclusion of the Euro VII limit. This evince that there is still a lot of work to be done.

Fortunately, Fig. 4b demonstrates that the incorporation of a 12 kW EGH allows the HDV to emit NOx below the Euro VI. Observe that all points in the map fulfil the Euro VI regulation. The Euro VII limit is also fulfilled except in a small region between 1000 − 1100 rpm and 60− 80% FTPP.

A more detailed analysis shows that NOx emissions achieved 3.83 g/kWh when the EGH was disabled at 1000 rpm and 60% FTPP. Under the same conditions, NOx measured with the EGH enabled, was about 0.46 g/kWh. This represents the maximum reduction found in all tests. In absolute terms, it represented a NOx reduction of 3.37 g/kWh. This, translated to relative terms, can be read as a 97.2% of NOx reduction at 50% FTPP.

Table 4
Stationary points selected for the tests.

Test	Engine regime (rpm)	FTPP (%)	Vehicle speed (km/h)
1	1000	30, 35, 40, 45, 50, 55, 60, 70, 80, 90	55
2	1250	30, 35, 40, 45, 50, 60, 70, 80, 90	68
3	1500	30, 35, 40, 45, 50, 60, 70, 80, 90	82

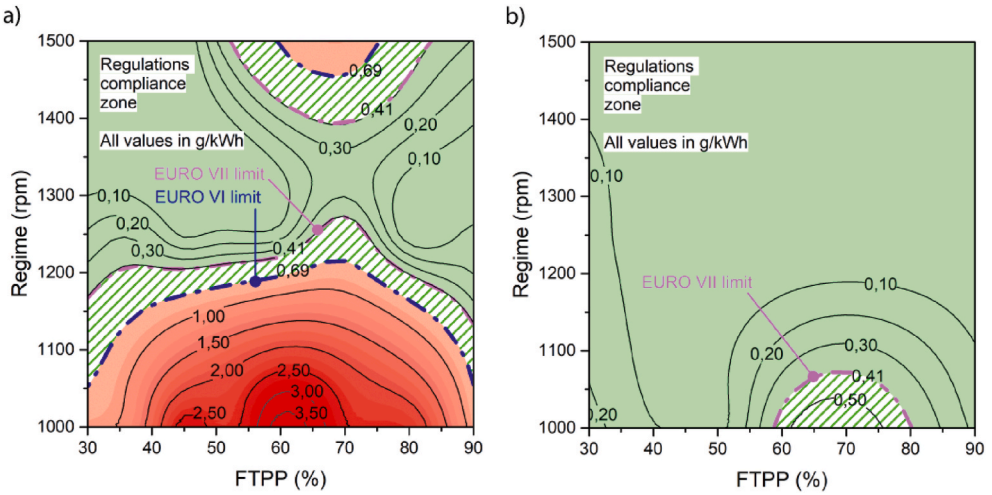

Fig. 4. NOx emissions map of a MAN TGX 18.480 Efficient Line 2 Euro VI HDV with the EGH a) disabled and b) enabled.

Considering the Euro VI scenario, note that all combinations of values in Fig. 4b are lower than the ISC limit value of 0.69 g/kWh. This means that the heat delivered by the EGH to exhaust gases was excessive to achieve the Euro VI limit, therefore, a smaller EGH could be used. The post Euro VI presented scenario (marked as Euro VII) is a little bit different because in some cases, the heat delivered by the EGH to exhaust gases was excessive (i.e. <0.41 g/kWh) and in other cases it was insufficient (i.e. > 0.41 g/kWh).

Fig. 5a and b shows the strictly necessary power required by the EGH to emit NOx below ISC limits, respectively. These values were obtained by interpolating the experimental values with the regulation limit. Note that the EGH power is not static because it depends on the temperature and mass flow rate of the exhaust gas. In both cases, the maximum power values delivered by the EGH are at 1000 rpm.

In Table 5, a comparison of the average power required by the EGH to emit NOx below ISC Euro VI and ISC Euro VII limits under three driving conditions are summarized. The most demanding regime is the suburban driving with an average EGH power requirement of 5.84 kW and 7.52 kW to accomplish ISC limits respectively. Furthermore, it is the most pollutant regime, emitting 10 times more NOx on average than the interurban driving and 7 times more compared with a highway driving.

Considering the time spent and the average NOx emissions at each driving condition in Table 5, it can be observed that the amount of NOx emitted during the suburban driving represents the 10% of the total NOx emitted during the mission. In other words, driving 4 min in suburban roads generates the same amount of NOx than driving 28 min in the highway. This justifies the need to focus on developing technologies that allow reducing NOx at this working regime. This is the purpose for which the TATH has been designed.

Table 5 also presents the average exhaust temperature and mass flow rate measured downwards the ATS. These values will be used in the following chapter to size and test the ATEG system. Note that, as also found in Ref. [19], it is not necessary to install a 12 kW EGH in a HDV to effectively reduce NOx emissions. Considering that the SCR light-off temperature for urea solution injection is 180 °C, it is demonstrated that the EGH device should only heat the exhaust gases to reach this target value. Provide extra thermal power to the

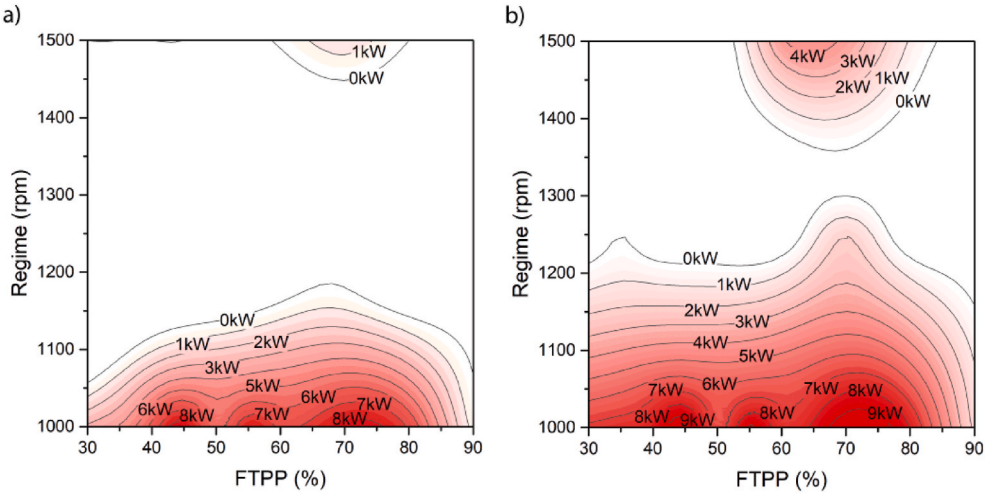

Fig. 5. EGH power demand map to emit NOx below a) ISC Euro VI and b) ISC Euro VII limits in a MAN TGX 18.480 Efficient Line 2 EURO VI HDV.

Table 5
Comparison of the average power required by the EGH under three driving conditions.

DRIVING CONDITION	Vehicle speed	Time[a]	Average NOx emissions of the standard ATS (g/kWh)	Average EGH power to fulfil ISC EURO VI limit $P_{EGH}^{EURO\ VI}$ (kW)	Average EGH power to fulfil ISC EURO VII limit $P_{EGH}^{EURO\ VII}$ (kW)	Average exhaust temperature downwards ATS (°C)	Average mass flow rate downwards ATS (kg/s)
SUBURBAN	55 km/h (1000 rpm)	1,5% (4 min)	2.09	5.84	7.52	159	0.147
INTERURBAN	68 km/h (1250 rpm)	0% (0 min)	0.19	0.00	0.22	228	0.172
HIGHWAY	82 km/h (1500 rpm)	98.5% (262 min)	0.30	0.19	0.95	196	0.204

[a] Taken from the real speed profile of a long-haul HDV presented in Fig. 2.

exhaust gases is unnecessary and counterproductive.

Finally, the EGH was tested in a hot air flow bench under the highway conditions to analyse its backpressure. The results from this test showed a maximum pressure loss of 1.8 mbar at 204 g/s. From this data, the hydraulic power, $P_{H_{EGH}} = Q_{EGH} \cdot \Delta p_{EGH}$, that the engine must provide to overcome the EGH additional back pressure is calculated. The greatest impact is presented in highway conditions with $P_{H_{EGH}} = \frac{0.204kg/s \cdot 180Pa}{0.745kg/m3} = 49.3\ W$.

4. ATEG experiment

Conventional internal combustion engine vehicles use an alternator to produce the electricity needed by the vehicle. This electricity is generated at expense of consuming more fuel. Some studies have reported that alternators are the responsible of 4 ∼ 6% of the total fuel consumption of the vehicle [29,32].

Most factory alternators for HDVs are available with outputs ranging from 160 up to 320 amps (3.84 kW–7.68 kW) and can handle the vehicle's basic necessities, such as headlights, gauges, fuel pumps, A/C, etc. Considering this power production range, the inclusion of a 5.84 kW EGH into the electrical system would require incorporating an exclusive alternator for the EGH, causing a significant increase in fuel consumption.

To avoid this extra fuel consumption, this chapter is focused on analysing the feasibility of using an ATEG as the main and only power supplier for the EGH. An ATEG is a heat recovery system designed to convert waste heat form exhaust gases into electricity. Many theoretical models [29,33–36] and experimental prototypes [31,37–40] have demonstrated the feasibility of ATEGs as on-board power suppliers.

4.1. ATEG experimental set up

The aim of this experiment is to find out how much power could be recovered from the exhaust fumes of a HDV, downstream of the ATS, under the real working conditions presented in Table 5. Fig. 6 shows the ATEG layout designed in this study. It has been engineered to feed the TATH electrical system based on the data collected in previous developments [29,31]. These studies demonstrated the importance of keeping the backpressure as low as possible to minimize the engine extra effort. Considering that, the proposed ATEG is composed by six ATEG single units (ATEG_su) arranged in parallel with respect to the fumes. Each one is identical to the one tested on [29]. The dimensions of the ATEG are 950x420 × 340mm (WxLxH), it weights around 40 kg and make use of 204 Bismuth Telluride thermoelectric modules.

To simplify the execution of the experiment, only one of the six ATEG_su was tested. The ATEG_su inlet temperatures and mass flow

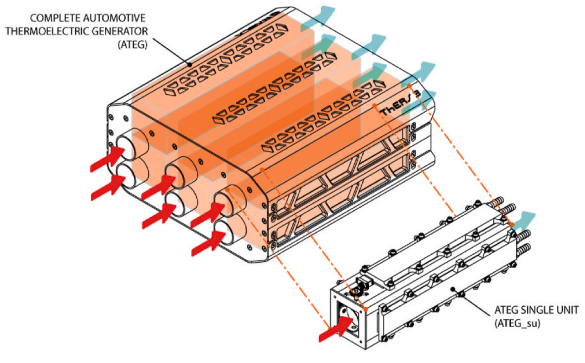

Fig. 6. Complete ATEG composed of six ATEG_su.

rates used in the experiment are presented on Table 7. Note that temperatures are quite similar to ones shown in Table 5. However, mass flow rates are one sixth of those described in Table 5, in order to consider the flow distribution.

Fig. 7a shows the ATEG_su with this cooling plate in first term and its connections to the cooling circuit. Fig. 7b presents the EGH coupled upstream to the ATEG_su. Inlet and outlet thermocouple sensors and the electrical power supply cable can also be seen.

The dimensions of the ATEG_su are 170x420 × 170mm (WxLxH) and weights around 8 kg without considering cooling fluid. It includes 34 thermoelectric modules (TEMs) configured in two parallel branches (of 8 and 9 individual TEMs) each one electrically connected in series. TEMs are composed of Bismuth Telluride, and they are assembled with graphite pads on their contact sides to provide low thermal resistance. Hot sides of these modules contact the surface of an aluminium heat exchanger, through which the exhaust gas flows. Cold sides are in contact with an aluminium plate with an interior cooling circuit. For more information about the ATEG_su, see Ref. [29].

Fig. 8 shows a scheme of the experimental bench used to test the ATEG_su coupled to a 12 kW EGH controlled by a PID. A chiller was used to emulate a real vehicle cooling system with temperature, flow rate, and pressure sensors. A pump was responsible of moving the water through the cold plates of the ATEG_su. Real operating conditions have been reproduced in the refrigeration circuit [29]. The energy generated by the ATEG_su was regulated and maximised by a converter and then stored to a 12V battery. A differential pressure sensor was used to register ATEG_su backpressure. Flow bench was coupled directly to the EGH inlet as seen in Fig. 10b. Table 6 shows relevant specifications related to used equipment in this experiment.

This equipment allows us to experiment with ATEGs cheaply and quickly. It allows us to modify the ATEG on the fly, a very interesting option when you are starting from an incipient and invalidated design. It also allows us to quickly set up any working regime and test ATEGs at small-scale without having to build the complete set. It is for this reason why, at this stage, we refused to do the test directly on the vehicle. All data collected in this study will minimize risks during the future design and construction of the complete TATH system. In this way it will be possible to face the future tests in a real vehicle with maximum guarantees.

4.2. ATEG experimental results

Table 7 shows the net power generation of the tested prototype in different real conditions. Note that the ATEG_su inlet mass flow rate is one sixth the average mass flow rate downwards ATS presented in Table 5.

From Table 7, it can be observed that the low exhaust temperatures at the end of the ATS generate a humble power production on the ATEG. Note that, with the increase of the exhaust gas temperature or mass flow rate, the power production also increases but exponentially. Consequently, it is recommended to thermally isolate the exhaust system in order to minimize heat losses upwards the ATEG. Fig. 9 shows the pressure drop of the ATEG_su under the three driving regimes. As seen in the figure, the curve fits to a linear function with a R-Square factor of 0.999.

5. Discussion

As explained in Chapter 3.2, the 10% of the total amount NOx produced during the mission was emitted during the suburban drive, which took the 1.5% of the mission time. These values demonstrate the need of a TATH system, which was designed to reduce these emissions at this regime. It heats up the exhaust gases only during the suburban driving and recover energy during the entire mission.

Once the performance of both, the EGH and the ATEG, have been obtained, it is the turn to analyse the capacity of the whole system to be energetically self-sufficient. To guarantee that the TATH system can feed itself autonomously, the energy consumed in the heating stage must be lower than the energy recovered, $E_{HEATING} \leq E_{RECOVERY}$. Eq. (1) details this relationship based on the parameters collected in the previous chapters.

$$0 \leq P_{ATEG_{HIGH}} t_{HIGH} + P_{ATEG_{INT}} t_{INT} + (P_{ATEG_{SUB}} - P_{EGH_{SUB}}) t_{SUB} \quad \text{Eq. 1}$$

where $P_{ATEG_{HIGH}}$, $P_{ATEG_{INT}}$ and $P_{ATEG_{SUB}}$ are the power recovered by the ATEG during the three driving conditions; and $P_{EGH_{SUB}}$ is the heating power of the EGH at suburban driving conditions. Finally, t_{HIGH}, t_{INT} and t_{SUB} are the times spent by the vehicle at highway, interurban and suburban routes, respectively. Those values are obtained using Eqs. (2)–(4).

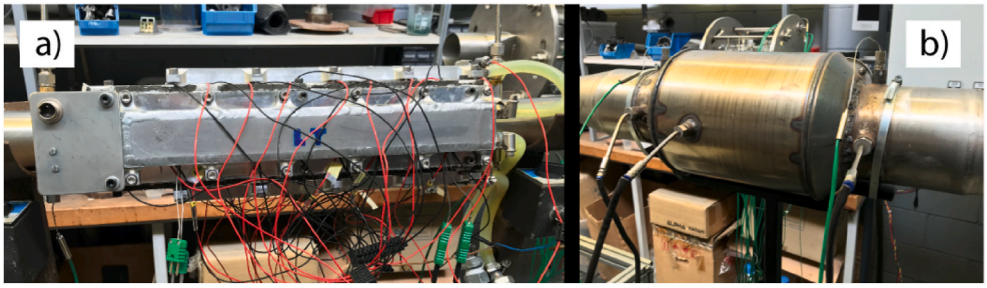

Fig. 7. a) ATEG_su prototype attached to the b) EGH.

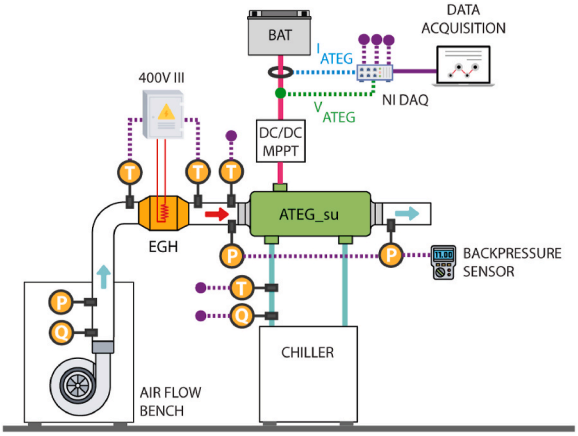

Fig. 8. Scheme of the test bench for ATEG_su.

Table 6
Detailed equipment specifications.

EQUIPMENT	MODEL	SPECIFICATIONS
Data acquisition system	National Instruments DAQ	Analogic and digital inputs Thermocouple slots Voltage: 0–10V and 0–60V Current: 0–5A
Chiller	Thermo Scientific ThermoChill II	Cooling temperature: 10 °C–30 °C Flow rate: 2.5 gpm @ 60 psid (9.4 lpm @ 4.1 bar) Accuracy: ±0.1 °C
Converter	Victron BlueSolar	130/35 DC/DC with MPPT
Pressure sensor	WIKA A2G-50	Accuracy: ±3%
Pump	SunSun NEO3800	Power consumption: 20W
Air Flow bench	Saenz J-600	Flow rate: up to 150 g/s Working temperature: 25 °C–400 °C

Table 7
Net power generation of an ATEG under three different driving conditions.

DRIVING CONDITION	Vehicle speed	Time*	ATEG inlet temperature (°C)	ATEG_su inlet mass flow rate (kg/s)	ATEG_su power generated (W)	ATEG power generated (W)	Hydraulic pump power (W)	ATEG net power generation P_{ATEG} (W)
SUBURBAN	55 km/h (1000 rpm)	1,5% (4 min)	162	0.025	23	138	20	118
INTERURBAN	68 km/h (1250 rpm)	0% (0 min)	225	0.028	34	204	20	184
HIGHWAY	82 km/h (1500 rpm)	98.5% (262 min)	210	0.035	53	318	20	298

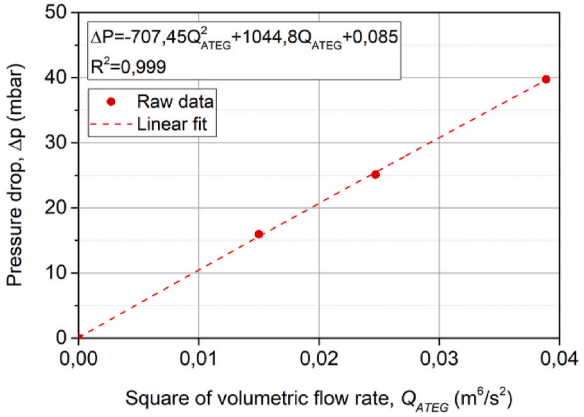

Fig. 9. ATEG_su pressure drop with respect to the square of volumetric flow rate.
Note that the maximum backpressure is 40 mbar at highway conditions. From this data, the hydraulic power, $P_{H_{ATEG}} = Q_{ATEG} \cdot \Delta p_{ATEG}$, that the engine must exert to overcome the back pressure is calculated. Note that Q_{ATEG} is the exhaust volumetric flow rate through the ATEG and Δp_{ATEG} the back pressure on the ATEG. The greatest impact occurs during highway conditions with $P_{H_{ATEG}} = \frac{0.204kg/s \cdot 4000Pa}{0.745kg/m3} = 1095.3\ W$.

Table 8
Time relationships to emit NOx below Euro VI and VII regulations in suburban conditions.

Scenario	Condition to emit NOx below ISC limit for suburban conditions	Percentage of time spent in suburban conditions with respect to mission time to emit NOx below Euro limit [%]
Euro VI	$0 \leq 298t_{HIGH} + 184t_{INT} - 5722t_{SUB}$	$t_{SUB\_MAX}^{EURO\ VI}$ <3.1–4.9%
Euro VII	$0 \leq 298t_{HIGH} + 184t_{INT} - 7402t_{SUB}$	$t_{SUB\_MAX}^{EURO\ VII}$ <2.4%–3.9%

$$t_{SUB} = \sum_{i=0}^{200} t_i = f(v)\ if\ v \leq \frac{50km}{h} \qquad \text{Eq. 2}$$

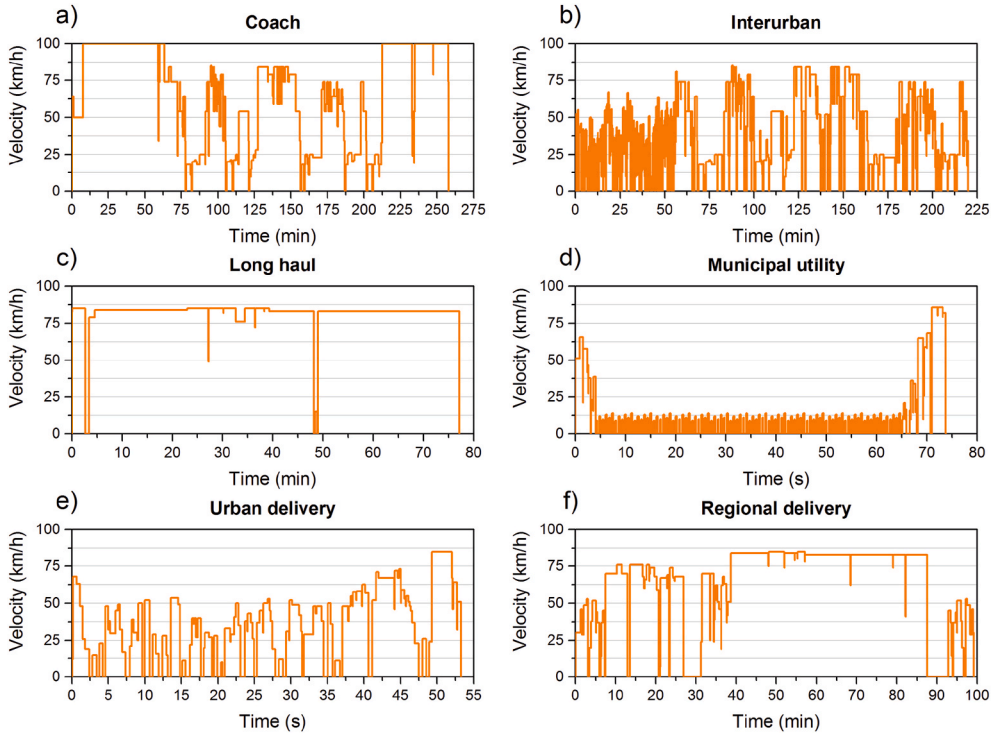

Fig. 10. Typical mission profiles of different HDVs.

$$t_{INT} = \sum_{i=0}^{200} t_i = f(v) \; if \; \frac{50km}{h} < v < \frac{80km}{h} \quad \text{Eq. 3}$$

$$t_{HIGH} = \sum_{i=0}^{200} t_i = f(v) \; if \; v \geq \frac{80km}{h} \quad \text{Eq. 4}$$

Substituting the power values by those obtained in Tables 5 and 7, the limit time relationships that satisfy the energy balance can be obtained. Table 8 conditions must be fulfilled to emit NOx below the desired ISC limits in suburban conditions. Note that these relations do not consider the power losses in the power converters, battery charge-discharge and regulation.

These equations demonstrate that, to achieve Euro VI NOx limit in suburban conditions, it is necessary that the HDV spends a maximum of 3.1% of the mission time in suburban conditions. This value is obtained considering that the recovery stage is exclusively limited to interurban driving. If the recovery stage is limited to highway conditions, this value is slightly higher, achieving a maximum of 4.9%. This can be explained by the higher power recovered in highway conditions compared to the same period in interurban conditions. A route that mixes highway and interurban driving would give an intermediate value between 3.1% and 4.9%. The same happens for Euro VII scenario presented, where this maximum stays between $2.4 - 3.9\%$, depending on the driving conditions during the recovery stage. Note that these two conditions are fulfilled in the long-haul mission profile described in Fig. 2, where the time spent in suburban conditions was 1.5%. Therefore, the incorporation of the TATH presented in this study would help a long-haul Euro VI HDV to reduce its NOx emissions below EURO VI and EURO VII limits only under suburban conditions.

However, the HDV usage or routing map is crucial in the viability of the TATH system. Fig. 10 shows six HDV mission profiles depending on the usage of the vehicle. These mission profiles have been extracted from VECTO software and reflect the current European fleet. VECTO is a simulation tool that has been developed by the European Commission and is used for determining CO_2 emissions and Fuel Consumption from Heavy Duty Vehicles (trucks, buses and coaches) with a Gross Vehicle Weight above 3500 kg.

From Fig. 10, the percentage of time spent in suburban conditions can be calculated with respect to the mission time, $r_{SUB} = 100 t_{SUB}/t_{MISSION}$, for each mission profile. Table 9 summarizes these values.

As explained in previous chapters, the maximum back pressure caused by the EGH and ATEG were 1.8 mbar and 40 mbar, respectively. This means that the TATH system increases the pressure drop in 41.8 mbar and the required engine power in $P_{H_{TATH}} = P_{H_{EGH}} + P_{H_{ATEG}} = 1144.3\ W$. Taking the power developed by the vehicle at that regime and the $P_{H_{TATH}}$, this would suppose a fuel consumption increase of 0.2%.

On the other hand, the additional weight that the TATH adds to the vehicle must also be considered. A heavier truck produces more rolling resistance than a lighter one, thereby increasing the power needed to move the vehicle. A 200 kg cut in vehicle weight can reduce fuel consumption by 0.5% on a regional delivery truck and 0.3% on a long haul truck [41]. Considering a TATH weight of 60 kg, this would suppose a fuel consumption increase of 0.09%. Other study [42] established that the average impact on mpg per tonne of increased payload of a HDV with a fuel consumption of 8.15 mpg is 0.112 mpg. This supposes a fuel consumption increase of 1.4% per tonne. In this case, the TATH would increase the fuel consumption by 0.08%. Besides, according to the fuel economy assessment method of ref. [33], the additional weight of the TATH would suppose an increase of 0.13% in fuel consumption.

Finally, the total fuel consumption increase due to the incorporation of TATH into the exhaust system would be 0.35%. It is clearly lower than the use of an exclusive alternator that supposes a 4–6% fuel consumption increase. With this information it can be concluded that the use of an ATEG is a better option than using an alternator to feed the TATH. Besides, the inclusion of the TATH into the exhaust system will not negatively affect the engine performance.

6. Conclusions

In this particular research, the use of a thermoelectric aftertreatment heater (TATH) to reduce NOx emissions of diesel-powered HDVs in low demanding regimes have been analysed. This system includes an Exhaust Gas Heater (EGH) that heats up the exhaust gases in low engine regimes, to shorten the time before urea is injected. Additionally, the TATH receives energy by an Automotive Thermoelectric Generator (ATEG) previously transforming wasted heat from exhaust gases into electricity, so the system can work

Table 9
Percentage of time spent in suburban conditions with respect the mission time for each mission profile.

Mission profile	r_{SUB}
Coach	25.02%
Interurban	44.15%
Long haul	0.64%
Municipal utility	32.74%
Urban delivery	48.65%
Regional delivery	11.20%

Note that only the long-haul mission profile satisfies the time requirements that makes the TATH system technically viable for both Euro regulations, $r_{SUB} < r_{SUB\_MAX}^{EURO\ VI}$ and $r_{SUB} < r_{SUB\_MAX}^{EURO\ VII}$. Long-haul transportation refers to a long-distance driving transportation system wherein the drivers undertake a single delivery by driving a commercial vehicle for a distance of 250 km or more. Typically, long-distance vehicles connect logistics centres that are close to major transportation routes, so they spend most of the journey on the highway. This is the reason why this type of vehicle is the most appropriate to incorporate the TATH system.

energetically independent.

This study demonstrates that under certain engine regimes, mainly at low-speed regimes, a Euro VI certified HDV emits NOx above the EURO VI limit. Note that this does not mean that the vehicle does not comply with EURO VI. The highest NOx emissions occur at regimes around 1000 rpm, which corresponds to suburban driving conditions. The highest value can be found at 1000 rpm and 60% FTPP, where NOx emission reached 3.83 g/kWh, 5 times higher than the regulatory limit.

One of the most significative findings is that the use of a TATH reduces NOx emissions by up to 97.2% in suburban regimes. TATH allows to a long-haul diesel-powered MAN Euro VI TGX 18.480 Efficient Line 2 to drastically reduce NOx emissions when driving in suburban conditions. The suburban driving is the most demanding regime with an average EGH power requirement of 5.84 kW and 7.52 kW to emit NOx below ISC Euro VI and Euro VII NOx limits in suburban conditions, respectively. It is also the most pollutant regime, emitting 7 times more NOx on average than the highway driving.

Besides, this study also demonstrates that an ATEG is capable to produce the energy required by the EGH in a long-haul mission profile. However, the added weight and the backpressure caused into the exhaust system increased the fuel consumption of the vehicle by 0.35%, which is lower than the expected of an exclusive alternator that would suppose a 4–6% fuel consumption increase.

To guarantee the energetic autonomy of the THAT, and to remain within the established emissions limit in suburban conditions, it is necessary for the HDV to spend a maximum of 3.1% of the mission time in suburban conditions, $r_{SUB\_MAX}^{EURO\ VI} = 3.1\%$. This value is obtained considering that the recovery stage occurs exclusively in interurban driving. If the recovery stage occurs only in highway conditions, this value is moderately higher, reaching a maximum of 4.9%, $r_{SUB\_MAX}^{EURO\ VI} = 4.9\%$. This can be explained by the fact that in highway conditions, the power recovered is higher than in interurban conditions. The same occurs for the most stringent scenario proposed, where r_{SUB} maximum remains between $r_{SUB\_MAX}^{EURO\ VII} = 2.4 - 3.9\%$, depending on the driving conditions of the recovery stage.

Finally, this study has demonstrated that the TATH can work energetically autonomous for long-haul HDVs. Among the vehicles analysed, long-distance transportation vehicles are the most appropriate to incorporate the TATH system due to the lower r_{SUB} ratio, which is $r_{SUB} = 0.64\% < r_{SUB\_MAX}^{EURO\ VI}$ and $< r_{SUB\_MAX}^{EURO\ VII}$. However, the viability of TATH could be extended to other HDV uses if the efficiency of ATEGs improved.

Declaration of competing interest

The authors declare that they have no known competing financial interests or personal relationships that could have appeared to influence the work reported in this paper.

Acknowledgments

We would like to thank Fundación Repsol and EVARM INNOVACION SL for their support.

Open Access funding provided thanks to the CRUE-CSIC agreement with Elsevier.

Eduard Massaguer is a Serra Húnter Fellow (tenure-track professor) in the Department of Mechanical Engineering and Industrial Construction at the University of Girona.

Albert Massaguer is a post-doctoral researcher in the Department of Mechanical Engineering and Industrial Construction at the University of Girona.

References

[1] Estimated cost of diesel emissions control technology to meet future Euro VII standards | International Council on Clean Transportation, (n.d.). https://theicct.org/publications/cost-diesel-emissions-control-euro-vii-apr2021 (accessed November 2, 2021).
[2] ACEA, Principles for Potential post-Euro 6 and post-Euro VI Emission Regulations, 2020.
[3] A. Noble, Next generation, EURO 7 Updat. Transp. Eng. (2017).
[4] AERIS Europe, Euro 7 impact assessment: the outlook for air quality compliance in the eu and the role of the road transport sector, 2021.
[5] V. Macián, J. Monsalve-Serrano, D. Villalta, Á. Fogué-Robles, Extending the potential of the dual-mode dual-fuel combustion towards the prospective EURO VII emissions limits using gasoline and OMEx, Energy Convers. Manag. 233 (2021), 113927, https://doi.org/10.1016/j.enconman.2021.113927.
[6] A. García, J. Monsalve-Serrano, D. Villalta, M. Guzmán-Mendoza, Methanol and OMEx as fuel candidates to fulfill the potential EURO VII emissions regulation under dual-mode dual-fuel combustion, Fuel 287 (2021) 119548, https://doi.org/10.1016/J.FUEL.2020.119548.
[7] T.& ENVIRONMENT, Road to Zero: the Last EU Emission Standard for Cars, Vans, Buses and Trucks, 2020.
[8] T. Grigoratos, G. Fontaras, B. Giechaskiel, N. Zacharof, Real world emissions performance of heavy-duty Euro VI diesel vehicles, Atmos. Environ. 201 (2019) 348–359, https://doi.org/10.1016/j.atmosenv.2018.12.042.
[9] R. Vermeulen, J. Spreen, N. Ligterink, W. Vonk, The Netherlands In-Service Emissions Testing Programme for Heavy-Duty, 2011.
[10] R. Vermeulen, W. Vonk, R. van Gijlswijk, The Netherlands In-Service Emissions Testing Programme for Heavy-Duty Vehicles 2015-2016-Annual Report, 2016.
[11] G.A. Bishop, B.G. Schuchmann, D.H. Stedman, Heavy-duty truck emissions in the south coast air basin of California, Environ. Sci. Technol. 47 (2013) 9523–9529, https://doi.org/10.1021/es401487b.
[12] M. Vojtisek-Lom, A.F. Arul Raj, P. Jindra, D. Macoun, M. Pechout, On-road detection of trucks with high NOx emissions from a patrol vehicle with on-board FTIR analyzer, Sci. Total Environ. 738 (2020), 139753, https://doi.org/10.1016/j.scitotenv.2020.139753.
[13] A.J. Kotz, D.B. Kittelson, W.F. Northrop, Lagrangian hotspots of in-use NOX emissions from transit buses, Environ. Sci. Technol. 50 (2016) 5750–5756, https://doi.org/10.1021/acs.est.6b00550.
[14] Y. Tan, P. Henderick, S. Yoon, J. Herner, T. Montes, K. Boriboonsomsin, K. Johnson, G. Scora, D. Sandez, T.D. Durbin, On-board sensor-based NOx emissions from heavy-duty diesel vehicles, Environ. Sci. Technol. 53 (2019) 5504–5511, https://doi.org/10.1021/acs.est.8b07048.
[15] F. Posada, H. Badshah, F. Rodriguez, In-Use NOx Emissions and Compliance Evaluation for Modern Heavy-Duty Vehicles in Europe and the United States, ICCT White Pap, 2020.
[16] L. He, J. Hu, S. Zhang, Y. Wu, X. Guo, J. Song, L. Zu, X. Zheng, X. Bao, Investigating real-world emissions of China's heavy-duty diesel trucks: can SCR effectively mitigate NOx emissions for highway trucks? Aerosol Air Qual. Res. 17 (2017) 2585–2594, https://doi.org/10.4209/aaqr.2016.12.0531.
[17] S. Ko, J. Park, H. Kim, G. Kang, J. Lee, J. Kim, J. Lee, NOx emissions from Euro 5 and Euro 6 heavy-duty diesel vehicles under real driving conditions, Energies 13 (2020), https://doi.org/10.3390/en13010218.

[18] G. Karavalakis, M. Hajbabaei, T.D. Durbin, K.C. Johnson, Z. Zheng, W.J. Miller, The effect of natural gas composition on the regulated emissions, gaseous toxic pollutants, and ultrafine particle number emissions from a refuse hauler vehicle, Energy 50 (2013) 280–291, https://doi.org/10.1016/j.energy.2012.10.044.
[19] J. Ximinis, A. Massaguer, T. Pujol, E. Massaguer, Nox emissions reduction analysis in a diesel Euro VI Heavy Duty vehicle using a thermoelectric generator and an exhaust heater, Fuel 301 (2021), 121029, https://doi.org/10.1016/j.fuel.2021.121029.
[20] O. Kröcher, Selective catalytic reduction of NOx, Catalysts 8 (2018) 459, https://doi.org/10.3390/catal8100459.
[21] W. Brack, B. Heine, F. Birkhold, M. Kruse, O. Deutschmann, Formation of urea-based deposits in an exhaust system: numerical predictions and experimental observations on a hot gas test bench, Emiss. Control Sci. Technol. 2 (2016) 115–123, https://doi.org/10.1007/s40825-016-0042-2.
[22] J. Han, J. Lee, Y. Oh, G. Cho, H. Kim, Effect of UWS injection at low exhaust gas temperature on NOx removal efficiency of diesel engine, Int. J. Automot. Technol. 18 (2017) 951–957, https://doi.org/10.1007/s12239-017-0093-6.
[23] M. Rink, G. Eigenberger, U. Nieken, Heat-integrated exhaust purification for natural gas engines, Chem. Ing. Tech. 85 (2013) 656–663, https://doi.org/10.1002/cite.201200162.
[24] M. Rink, G. Eigenberger, U. Nieken, Comparison of two different heat-integrated exhaust purification devices for monovalent CNG engines, Top. Catal. 56 (2013) 421–426, https://doi.org/10.1007/s11244-013-9990-8.
[25] Z. Mera, C. Matzer, S. Hausberger, N. Fonseca, Performance of selective catalytic reduction (SCR) system in a diesel passenger car under real-world conditions, Appl. Therm. Eng. 181 (2020), 115983, https://doi.org/10.1016/j.applthermaleng.2020.115983.
[26] D. Culbertson, M. Khair, S. Zhang, J. Tan, J. Spooler, The study of exhaust heating to improve SCR cold start performance, SAE Int. J. Engines. 8 (2015), https://doi.org/10.4271/2015-01-1027.
[27] C. Sharp, C.C. Webb, S. Yoon, M. Carter, C. Henry, Achieving ultra low NOX emissions levels with a 2017 heavy-duty on-highway TC diesel engine - comparison of advanced technology approaches, SAE Int. J. Engines. 10 (2017) 1722–1735, https://doi.org/10.4271/2017-01-0956.
[28] A. Massaguer, T. Pujol, M. Comamala, E. Massaguer, Feasibility study on a vehicular thermoelectric generator coupled to an exhaust gas heater to improve aftertreatment's efficiency in cold-starts, Appl. Therm. Eng. 167 (2020), 114702, https://doi.org/10.1016/j.applthermaleng.2019.114702.
[29] E. Massaguer, A. Massaguer, T. Pujol, M. Comamala, L. Montoro, J.R. Gonzalez, Fuel economy analysis under a WLTP cycle on a mid-size vehicle equipped with a thermoelectric energy recovery system, Energy 179 (2019) 306–314, https://doi.org/10.1016/j.energy.2019.05.004.
[30] E. Massaguer, A. Massaguer, E. Balló, I.R. Cózar, T. Pujol, L. Montoro, M. Comamala, Electrical generation of a ground-level solar thermoelectric generator: experimental tests and one-year cycle simulation, Energies 13 (2020), https://doi.org/10.3390/en13133407.
[31] A. Massaguer, E. Massaguer, M. Comamala, T. Pujol, L. Montoro, M.D. Cardenas, D. Carbonell, A.J. Bueno, Transient behavior under a normalized driving cycle of an automotive thermoelectric generator, Appl. Energy 206 (2017) 1282–1296, https://doi.org/10.1016/j.apenergy.2017.10.015.
[32] L.C.M. Sales, E.P. Pacheco, L.G.C. Monteiro, L.G. Souza, M.S. Mota, Evaluation of the influence of an alternator with mechanical decoupling on energy consumption and CO_2 emission in a flex fuel vehicle, SAE Tech. Pap. (2017), https://doi.org/10.4271/2017-36-0116, 2017-November.
[33] A. Massaguer, E. Massaguer, M. Comamala, T. Pujol, J.R. González, M.D. Cardenas, D. Carbonell, A.J. Bueno, A method to assess the fuel economy of automotive thermoelectric generators, Appl. Energy 222 (2018) 42–58, https://doi.org/10.1016/j.apenergy.2018.03.169.
[34] S. Lan, Z. Yang, R. Stobart, R. Chen, Prediction of the fuel economy potential for a skutterudite thermoelectric generator in light-duty vehicle applications, Appl. Energy 231 (2018) 68–79, https://doi.org/10.1016/j.apenergy.2018.09.087.
[35] Z.G. Shen, L.L. Tian, X. Liu, Automotive exhaust thermoelectric generators: current status, challenges and future prospects, Energy Convers. Manag. 195 (2019) 1138–1173, https://doi.org/10.1016/j.enconman.2019.05.087.
[36] E. Massaguer, A. Massaguer, T. Pujol, J.R. Gonzalez, L. Montoro, Modelling and analysis of longitudinal thermoelectric energy harvesters considering series-parallel interconnection effect, Energy 129 (2017) 59–69, https://doi.org/10.1016/j.energy.2017.04.061.
[37] M. Comamala, T. Pujol, I.R. Cózar, E. Massaguer, A. Massaguer, Power and fuel economy of a radial automotive thermoelectric generator: experimental and numerical studies, Energies 11 (2018), https://doi.org/10.3390/en11102720.
[38] M. Comamala, I.R. Cózar, A. Massaguer, E. Massaguer, T. Pujol, Effects of design parameters on fuel economy and output power in an automotive thermoelectric generator, Energies 11 (2018) 3274, https://doi.org/10.3390/en11123274.
[39] P. Fernández-Yañez, O. Armas, A. Capetillo, S. Martínez-Martínez, Thermal analysis of a thermoelectric generator for light-duty diesel engines, Appl. Energy 226 (2018) 690–702, https://doi.org/10.1016/j.apenergy.2018.05.114.
[40] A. Marvão, P.J. Coelho, H.C. Rodrigues, Optimization of a thermoelectric generator for heavy-duty vehicles, Energy Convers. Manag. 179 (2019) 178–191, https://doi.org/10.1016/j.enconman.2018.10.045.
[41] Fuel efficiency technology in European heavy-duty vehicles: baseline and potential for the 2020–2030 timeframe | International Council on Clean Transportation, n.d. https://theicct.org/publications/fuel-efficiency-technology-european-heavy-duty-vehicles-baseline-and-potential-2020. (Accessed 28 October 2021).
[42] M. Coyle, Effects of payload on the fuel consumption of trucks, 2007.